Fracture properties of high-entropy alloys

Bernd Gludovatz* and Robert O. Ritchie

Since the concept of high-entropy alloys (HEAs) as materials with at least four or five principal elements in (near)-equiatomic composition was introduced in 2004, this new class of materials has penetrated essentially all materials science-related fields. The main reason for this is that some face-centered-cubic alloy compositions have been shown to exhibit truly outstanding mechanical properties with extraordinary combinations of strength, ductility, and fracture toughness, particularly at cryogenic temperatures, whereas certain body-centered-cubic refractory compositions display remarkable high-temperature strength. While significant efforts have been put into rapid screening and narrowing the compositional space of HEAs to a manageable scope, there are still only a few metallic alloys that push the limits of mechanical performance. Here, we review work on some of the most damage-tolerant HEAs discovered to date and discuss the fundamental reasons why their resistance to fracture and subsequent stable crack growth is so exceptional.

Introduction

In the past decades, significant progress has been made in our understanding of the relationships between processing, microstructure, and mechanical properties of advanced materials for structural applications, thereby enabling the development of damage-tolerant materials with outstanding combinations of strength, ductility, and failure resistance. Despite the ongoing development of new characterization techniques that allow the identification and understanding of deformation mechanisms at unprecedented levels to uncover the structure–property relationships of new materials, major shifts away from the classical alloy design where metallic alloys invariably involve a single dominant element, such as iron in steels and nickel in superalloys, are scarce. Bulk-metallic glasses (BMGs) and high-entropy alloys (HEAs), however, represent a radical departure from these notions. BMGs are multicomponent materials that have been worked on extensively since the late 1980s and exhibit outstanding strength and elastic properties which make them tantalizing prospects for many engineering applications.[1–3] Nevertheless, our poor understanding of how their amorphous structure controls mechanical performance together with limitations in processing of BMGs has impeded our ability to apply materials science principles in their design and consider them for many structural applications.[4–7] HEAs, on the other hand, are, by definition, equiatomic, multi-element metallic systems that contain high concentrations of different elements.[8–10] They represent a new field of metallurgy that focuses attention away from the corners of alloy phase diagrams toward their centers, thereby enabling numerous combinations of new materials. While early research on HEAs has focused on systems containing at least five elements in equiatomic ratios that can crystallize as a single phase,[8,9] the definition of a HEA has been extended to contain high concentrations (5–35 at.%) of multiple elements that form materials with simple crystal structures.[11] This has opened the field to enable research into numerous applications so that, in less than two decades, HEAs have transitioned from a small research direction to a major field in materials science with work ranging from alloy design to atomic ordering phenomena.[12] Despite the enormous interest in these materials, only few new alloy compositions have been identified which push the limitations in mechanical performance of state-of-the-art structural materials. One of the reasons for this is that many new alloys that appear to be promising candidates for structural applications have either been characterized in their as-cast conditions or using compression testing only. Despite

Bernd Gludovatz, School of Mechanical and Manufacturing Engineering, University of New South Wales (UNSW Sydney), Australia; b.gludovatz@unsw.edu.au
Robert O. Ritchie, Materials Sciences Division, Lawrence Berkeley National Laboratory, and Department of Materials Science and Engineering, University of California, USA; roritchie@lbl.gov
*Corresponding author
doi:10.1557/s43577-022-00267-9

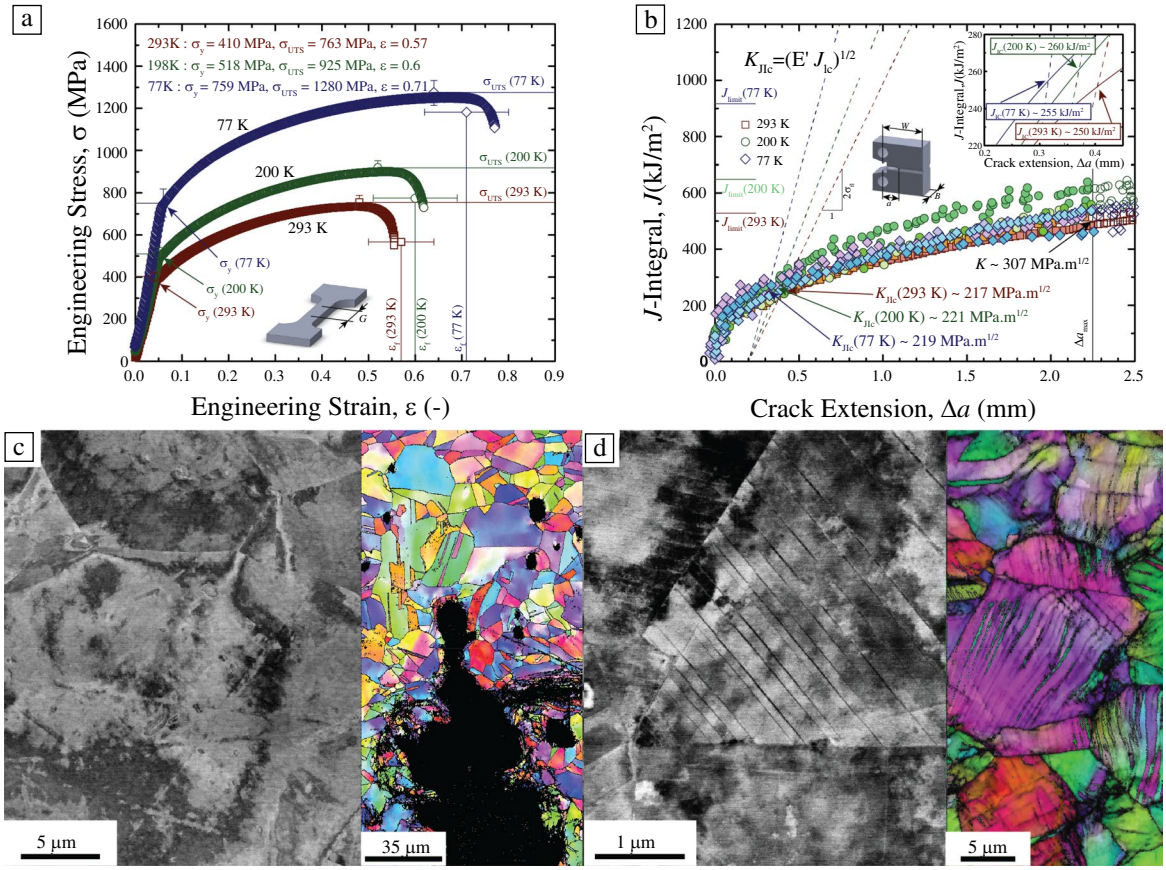

Figure 1. Strength, fracture toughness, and deformation mechanisms in the CrMnFeCoNi HEA. (a) Tensile stress–strain behavior in the range of room (293 K) to liquid-nitrogen (77 K) temperatures showed increasing yield and ultimate tensile strength, as well as increasing failure strains with decreasing temperature. (b) *J*-based crack-resistance curve testing revealed increasing crack-propagation resistance with crack extension and fracture toughness, K_{Jlc} values of ~220 MPa $m^{1/2}$ at all temperatures. (c) Failure at room temperature can be associated with dislocation motion resulting in dislocation cell structure formation that is apparent from grain misorientations within individual grains. (d) Back-scattered electron microscopy together with electron back-scattered diffraction maps revealed nanoscale deformation twinning as an additional deformation mechanism at 77 K.[16]

some promising results, the obtained microstructure–mechanical property relationships are known to often provide a false proxy for mechanical performance as they ignore difficulties with malleability, the impact of thermomechanical processing after casting, and the importance of a well-defined microstructure. Rapid screening methodologies for new alloy compositions that show promise as materials for structural applications, on the other hand, often lack the ability to isolate metastable conditions that may be of scientific interest or identify materials that can be thermomechanically processed into technologically viable products.

In this work, we review the mechanical properties, particularly in terms of fracture behavior, of some of the most notable and damage-tolerant HEAs that have been identified to date. We highlight examples of equiatomic materials, both face-centered cubic (fcc) and body-centered cubic (bcc), as well as alloy compositions that are off equimolar stoichiometry. We focus on the mechanisms underlying their resistance to failure after being thermomechanically processed and discuss the importance of fracture toughness in the design and use of damage-tolerant HEAs.

Strength, ductility, and fracture toughness of equiatomic, single-phase HEAs

The first, and one of only a few HEAs that has been characterized in terms of fracture toughness and crack-propagation resistance to date, is the fcc-structured, single-phase HEA CrMnFeCoNi. The alloy, which is undoubtably the most studied HEA today, was introduced by Cantor et al. in 2004[8] and has subsequently been processed and extensively characterized by George and co-workers at Oak Ridge National Laboratory (ORNL) from 2008 onward.[13] At room temperature, uniaxial tensile tests on recrystallized material with equiaxed grains in the range of ~4 to 160 μm showed a yield strength, σ_y of ~200 to 350 MPa, an ultimate tensile strength, σ_{UTS} between ~550 and 650 MPa, and ductility with strain to failure, ε_f of ~0.6 to

0.8.[14,15] Elevated temperature tests up to 1073 K revealed progressively decreasing σ_y and σ_{UTS} with increasing temperature; similarly, ε_f degraded with temperature for the coarser-grained materials but was comparable to room-temperature values for the finer-grained materials.[15] Additional tests between room (293 K) and liquid-nitrogen temperatures (77 K) were conducted due to the single-phase character of the alloy. In this temperature range, the material simultaneously showed a significant increase in σ_y, σ_{UTS}, and ε_f with decreasing temperature, as shown for tests on recrystallized material with ~6-mm grain size in **Figure** 1a.[14–16] For this batch, specifically, σ_y increased from ~410 to 760 MPa, σ_{UTS} from 760 to 1280 MPa, and ε_f from 0.57 to 0.71; while these values are comparable to the previously tested material,[14,15] small differences in the obtained results may be associated with compositional variations and effects of ordering phenomena that have recently been shown to exist in some CrCoNi-based HEAs.[17–19] At all temperatures, deformation at small strains was characterized by planar glide of 1/2<110> dislocations on {111} planes, with the motion of Shockley partial dislocations and the concomitant generation of stacking faults apparent at higher strains. At room temperature and above, this resulted in the formation of cell structures, whereas below 293 K, nanoscale deformation twinning was observed as additional deformation mechanisms at strains of 20% or more.[15] Over the entire temperature range, this resulted in pronounced work hardening with a strain-hardening exponent, n of ~0.4.[15,16] Such strong temperature dependence of σ_y and σ_{UTS} together with the substantial change in ε_f is not typically observed in pure fcc metals and runs counter to most other materials where an inverse dependence of ductility and strength is invariably seen.[20] The results of these sub-zero temperature tests in many respects triggered the immense interest of the structural materials community in HEAs.

Based on the tensile properties, fracture toughness tests were conducted on the ~6-μm grain size material batch using precracked and side-grooved compact-tension, C(T) samples between room and liquid-nitrogen temperatures.[16] Despite the significant increase in strength with decreasing temperature, the crack-initiation toughness, K_i at first crack extension for both 293 K and 77 K, was close to ~200 MPa $m^{1/2}$, and fracture toughness, K_{JIc}, determined according to the ASTM-standard[21] from the intersection with the blunting lines at 200-μm crack extension, was ~220 MPa $m^{1/2}$ (J_{Ic} ~ 255 kJ m^{-2}) at all testing temperatures, as shown in Figure 1b. Furthermore, over the entire temperature range, the material showed similar crack-growth characteristics with rising crack-resistance curve (R-curve) behavior to stress intensity, K values in excess of 300 MPa $m^{1/2}$ (J ~ 500 kJ m^{-2}) at ~2.25-mm crack extension. Fractographic analyses after testing revealed fully ductile fracture with microvoids initiating at either Cr- or Mn-rich particles that were found inside numerous dimples across the fracture surfaces. Similar to the tensile tests, backscattered electron (BSE) microscopy and electron back-scatter diffraction (EBSD) scans showed dislocation cell structure formation at room temperature (Figure 1c), which together with nanoscale deformation twinning at 77 K (Figure 1d) resulted

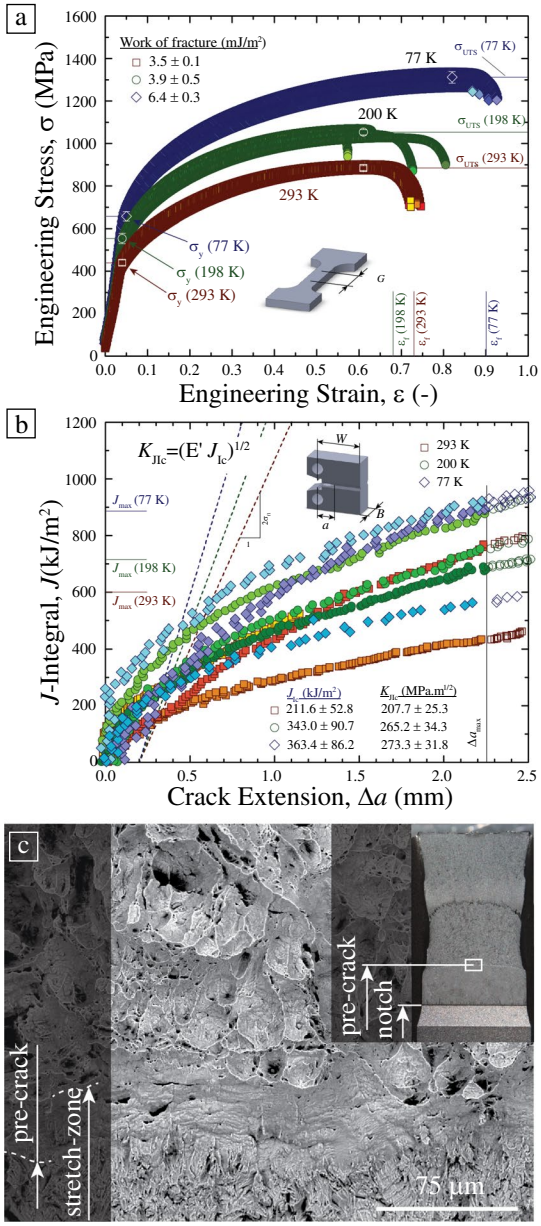

Figure 2. Mechanical properties and damage tolerance of the CrCoNi alloy. (a) Tensile stress–strain testing using dog bone-shape samples revealed a significant increase in strength, ductility, and fracture toughness from room (293 K) to liquid-nitrogen (77 K) temperatures. In the same temperature range, work of fracture increased from 3.5 ± 0.1 mJ/m^2 at 293 K to 6.4 ± 0.3 mJ/m^2 at 77 K. (b) Crack-resistance curves exhibited an increasing crack-propagation resistance with crack extension and crack-initiation toughness values of ~200–270 MPa $m^{1/2}$ for all tested temperatures. (c) Failure was associated with fully ductile dimple fracture initiating from the pre-crack via a pronounced stretch zone and microvoid coalescence upon further crack extension.[22]

in extensive plasticity leading to the outstanding fracture toughness and the pronounced crack-resistance curve behavior of the CrMnFeCoNi HEA at room temperature and below.[16]

Medium-entropy alloys and fcc HEAs with non-equimolar stoichiometry

The only other material that has been studied in terms of damage tolerance including fracture toughness and *R*-curve behavior is the medium-entropy alloy (MEA) CrCoNi.[22] While the material has been shown to exhibit failure characteristics that are comparable to the Cantor alloy, many of its mechanical properties exceed those of the five-component alloy.[16,22] In terms of strength, tensile tests on recrystallized material with equiaxed grains in the range of ~5 to 50 μm showed a ~50% increase in both σ_y and σ_{UTS} to ~660 MPa and ~1300 MPa, respectively, and a ~25% increase in ε_f to ~0.9 with decreasing temperature from 293 to 77 K, as shown in **Figure** 2a; the work-hardening rate at all testing temperatures was comparable to the Cantor material with $n \sim 0.4$.[22] *R*-curve testing (Figure 2b) revealed K_{JIc} values of ~210 MPa $m^{1/2}$ (J_{Ic} ~ 210 kJ m^{-2}) at room temperature, whereas at 77 K, a fracture toughness, K_{JIc} of ~275 MPa $m^{1/2}$ (J_{Ic} ~ 265 kJ m^{-2}) was measured; all fracture toughness numbers were valid by ASTM standards.[21] Akin to the five-component alloy, the fracture behavior at all temperatures was associated with ductile fracture resulting in a pronounced stretch zone at crack initiation followed by failure by microvoid coalescence (Figure 2c). While minor amounts of a hexagonal close-packed (hcp) minority phase may affect the mechanical performance of this alloy,[23] the main reason for its outstanding damage tolerance has been associated with a ~25% lower stacking-fault energy (SFE) of 22 ± 4 mJ m^{-2} compared to the FeMnCoNiCr but a comparable critical resolved shear stress (CRSS).[24] As a result, the twinning stress in the CrCoNi alloy is reached at lower strains causing the onset of nanoscale deformation twinning at room temperature and an extended range of extensive and steady work hardening leading to the extraordinary mechanical performance.[24]

The outstanding ductility and fracture toughness together with notable fatigue strength[28–30] of both the CrMnFeCoNi and CrCoNi alloys put them among the most damage-tolerant materials with fcc crystal structure to date, comparable with austenitic stainless steels,[31,32] high-Ni,[33–39] and high-Mn steels[40–43] for cryogenic applications. With their high lattice friction and low stacking-fault energy, this is primarily a result of the generation of a synergistic sequence of deformation mechanisms—dislocation glide, stacking-fault generation, twinning-induced plasticity (TWIP), and transformation-induced plasticity (TRIP)—which leads to continuous strain hardening, which obviously hardens the material yet at the same time delays the necking instability to enhance ductility. As these processes can become even more effective at cryogenic temperatures, particularly deformation twinning, coupled with the lack of any ductile-to-brittle transition, these fcc HEAs can be more damage tolerant at lower temperatures.

Nevertheless, their main drawback is their low yield strength. Among various alloying strategies, lowering the stacking-fault energy by reducing the Mn content while simultaneously increasing Fe content to promote deformation mechanisms has resulted in non-equiatomic TWIP and TRIP HEAs, and ultimately dual-phase (DP) HEAs that contained, in addition to the fcc phase, an hcp phase, as shown in **Figure** 3a;[25] it should be noted that compared to the Cantor material, none of the alloys in this study contained Ni. Despite their outstanding strain-hardening potential, gains in yield strength have only been limited. Moreover, the TRIP effect can certainly elevate the strain hardening but the resultant hcp ε-martensite is quite brittle, especially at cryogenic temperatures.[44] Alternative alloying strategies such as reducing and/or replacing individual elements (e.g., Cr with V), thereby utilizing lattice distortion as a core effect in the design of HEAs, have, however, proven to be significantly more effective in changing σ_y.[26] A $Ni_{63.2}V_{36.8}$ alloy, for example, has shown an increase in yield strength above 700 MPa compared to ~400 MPa for the CrMnFeCoNi alloy and ~500 MPa for the CrCoNi alloy[27]; alloy comparisons were made for materials with similar grain sizes around ~6–8 mm. Similarly, a CoNiV alloy has been designed with $\sigma_y \sim 550$ MPa, which can further be increased up to approximately 1 GPa through grain size reduction down to ~2 mm; importantly, the resulting gains in yield strength were only slightly compromised by moderate reductions in ductility (Figure 3b).[26]

Despite the outstanding strength-ductility properties of these materials, their damage tolerance and failure resistance remain somewhat uncertain particularly due to the lack of tests on samples that contain a crack. Admittedly, for alloys with low yield strength but outstanding ductility, such as the CrMnFeCoNi alloy, the critical factor for their use in structural applications, aside from cost, is still likely to be their strength, but increasing strength in most metallic materials is invariably associated with reductions in ductility, as shown for example for the CoNiV alloy.[26] Given that most materials exhibit this trend of a tradeoff between strength versus ductility and toughness,[20] the true potential of the fcc HEAs is that they can achieve a high (ultimate) tensile strength together with an increase in tensile ductility, which leads to their exceptional resistance to fracture.

Strength and ductility in bcc RHEAs

Multiple principal element alloys also present unique opportunities to make significant gains with a bcc structure in the form of refractory high/medium-entropy alloys (RHEAs) which are aimed at ultrahigh temperature applications[45–48] or applications requiring radiation-tolerant materials.[49,50] Early work on RHEAs by Senkov and co-workers, for example, has shown that $Nb_{25}Mo_{25}Ta_{25}W_{25}$ and $V_{20}Nb_{20}Mo_{20}Ta_{20}W_{20}$ alloys can exhibit excellent combinations of strength and ductility (**Figure** 4a–d),[46] but unfortunately, like most testing on RHEAs, this was performed in compression. At room temperature, both of these HEAs have a yield strength in

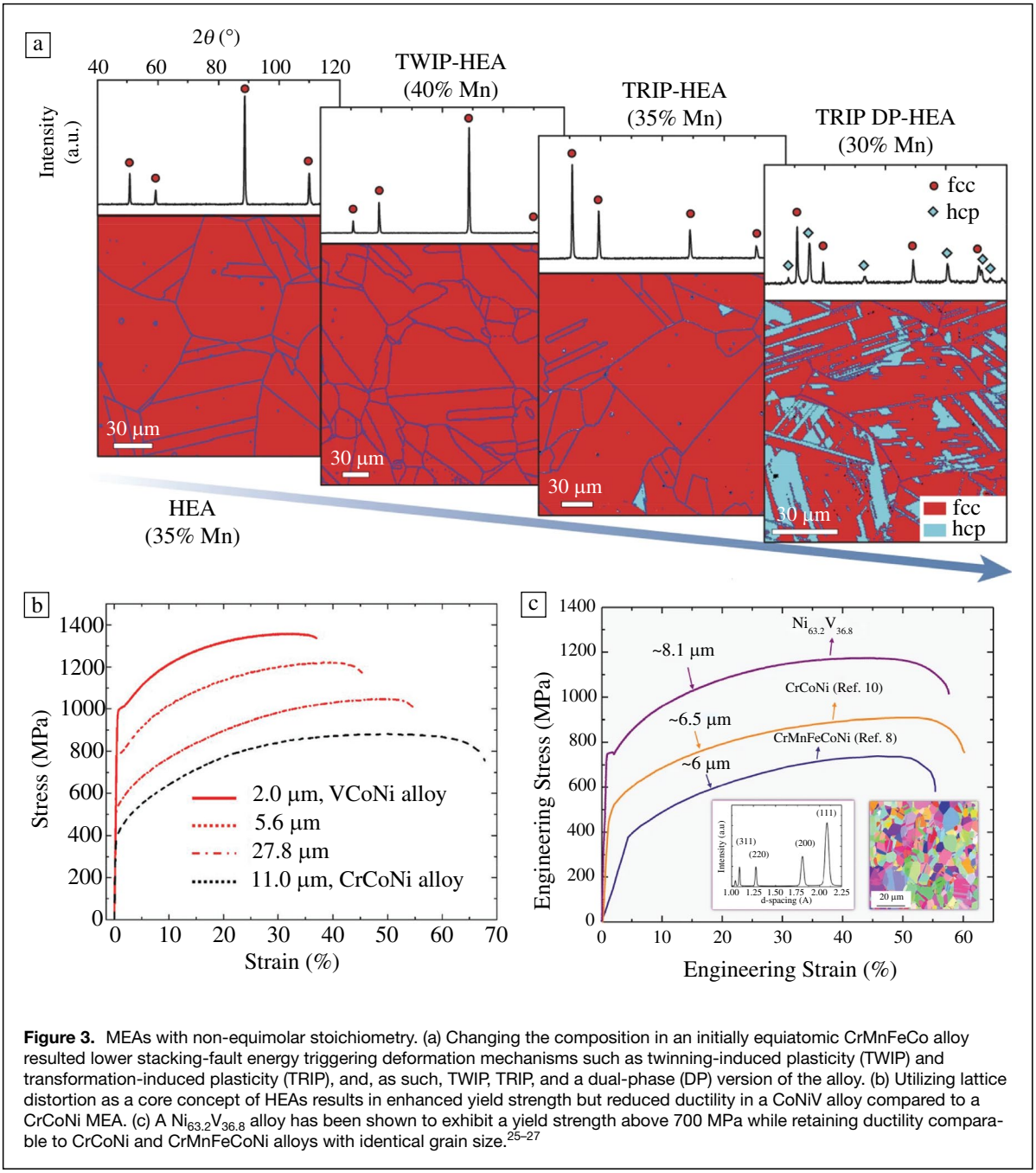

Figure 3. MEAs with non-equimolar stoichiometry. (a) Changing the composition in an initially equiatomic CrMnFeCo alloy resulted lower stacking-fault energy triggering deformation mechanisms such as twinning-induced plasticity (TWIP) and transformation-induced plasticity (TRIP), and, as such, TWIP, TRIP, and a dual-phase (DP) version of the alloy. (b) Utilizing lattice distortion as a core concept of HEAs results in enhanced yield strength but reduced ductility in a CoNiV alloy compared to a CrCoNi MEA. (c) A $Ni_{63.2}V_{36.8}$ alloy has been shown to exhibit a yield strength above 700 MPa while retaining ductility comparable to CrCoNi and CrMnFeCoNi alloys with identical grain size.[25–27]

excess of 1 GPa and ductilities of about 2% failure strains (Figure 4a, c), whereas at elevated testing temperatures up to 1000°C they demonstrated excellent plastic flow properties exceeding ~ 10–15% strains (Figure 4b, d). Moreover, both materials remain disordered and stable up to 1400°C. While testing of these materials was performed in the as-cast condition, some properties compare favorably to conventional superalloys making these alloy compositions attractive for further exploration of subsequent thermomechanical processing routes and assessment of corresponding mechanical performance. The most prominent bcc RHEA to date, however, is undoubtably the alloy TiZrNbHfTa. Compared to the NbMoTaW-based RHEAs, this alloy has been tested at room temperature after hot isostatic pressing (HIP) to show a compressive yield strength close to 1 GPa and failure strengths in excess of 2 GPa with ductilities above 50%, as shown in Figure 4e.[51] At elevated-temperature tests between 296 and 873 K, the material shows temperature-independent strain hardening through deformation twinning and shear-band formation;[47] above this temperature, however, σ_y drops below ~ 500 MPa. Importantly, this material has additionally been tested in tension after high-pressure torsion (HPT)

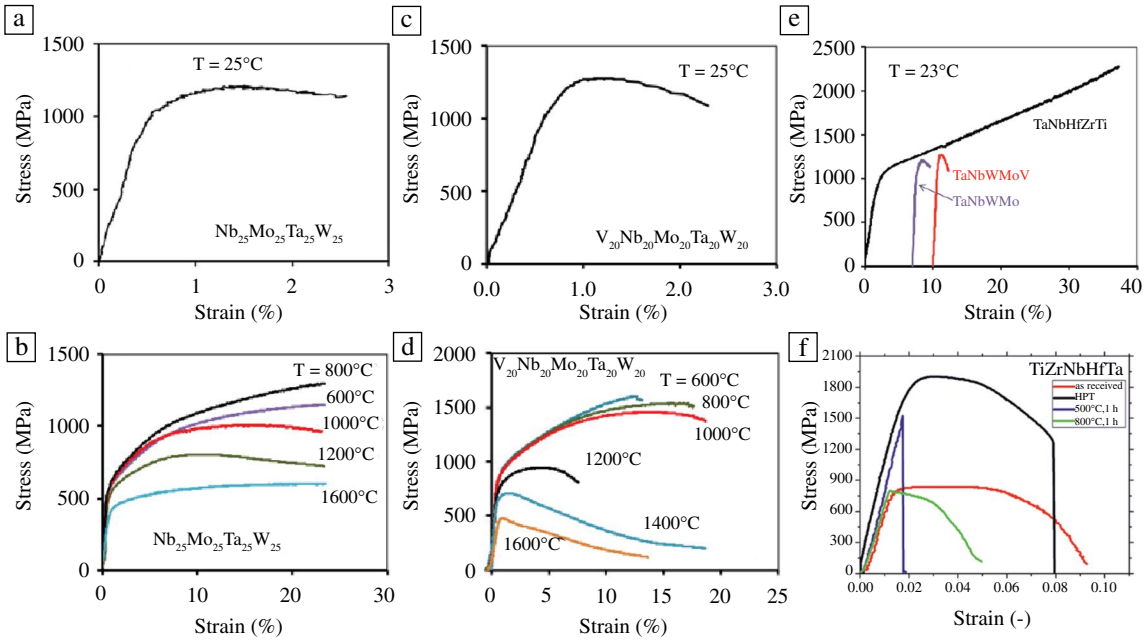

Figure 4. Stress–strain response of bcc RHEAs. Compression testing of (a, b) a NbMoTaW alloy and (c, d) a VNbMoTaW alloy at (a, c) room temperature and (b, d) elevated temperatures up to 1600°C showed increasing ductility and decreasing yield strength with increasing temperature for both materials. (e) Compared to that, a TaNbHfZrTi alloy displayed somewhat lower yield strength but significantly more ductility in compression, whereas (f) in tension, the alloy exhibited failure strains close to 10% in the as-received condition. Upon grain refinement, the material loses ductility while strength increases up to ~1.9 GPa.[46,51,52]

deformation with results compared to coarse-grained material with ~100-mm grain size.[52] While the coarse-grained material exhibited a yield strength of ~700 MPa and failure strains of ~9%, HPT deformation resulted in ~50 to 100-nm grain size, σ_y in excess of ~1800 MPa and ε_f ~ 8 percent. Even after irradiation with He^{2+} ions, the material remained highly ductile with ε_f ~ 5% while simultaneously increasing $\sigma_y > 2$ GPa.[49] This not only highlights the outstanding performance of the TiZrNbHfTa HEA in both compression and tension but also shows the potential of bcc-HEAs for high-temperature applications and as materials that require irradiation damage tolerance.

Neither of the aforementioned alloys has been evaluated in terms of their failure resistance which is mainly due to issues with processing and malleability into sufficiently sized samples with a somewhat homogeneous grain structure. Despite the difficulties with thermomechanically designing microstructures that can withstand many of the demanding requirements of high-temperature applications or irradiation, recent successes in the design of alloy compositions that appear to show tensile ductility in either as-cast[53] or thermomechanically processed conditions,[54] together with processing techniques such as additive manufacturing appear to demonstrate promising pathways for engineering future damage-tolerant multiple principal element alloys. For the bcc RHEAs, which invariably display high strength but limited ductility, characterization using tensile tests and especially fracture toughness testing at both ambient and elevated temperatures is imperative if these materials are ever to be realistically considered for structural applications. In stark contrast to the fcc HEAs where the K_{Ic} toughness values can be measured in the hundreds of MPa $m^{1/2}$, it is the authors' (unpublished) experience with the bcc RHEAs that the corresponding K_{Ic} values, at both low and high temperatures, are generally in the single digits. Despite the plethora of publications that emerge each week devoted to HEAs, this is definitively an area where extensive research is really needed.

Damage tolerance in compositionally complex multi-phase materials

The most damage-tolerant MEA/HEA-type materials to date are compositionally complex multi-phase materials. Despite their structures being somewhat far from the original concept of a high-entropy alloy, their mechanical properties, particularly their tensile stress–strain response, highlight not only the effect of widening the field to multi-phase systems but provide an outlook at the true potential of compositionally complex materials.

Of the many multi-phase alloys that have been discovered and reported in the past years, the best performing material, so far, has been introduced in 2018 by Liu and co-workers,

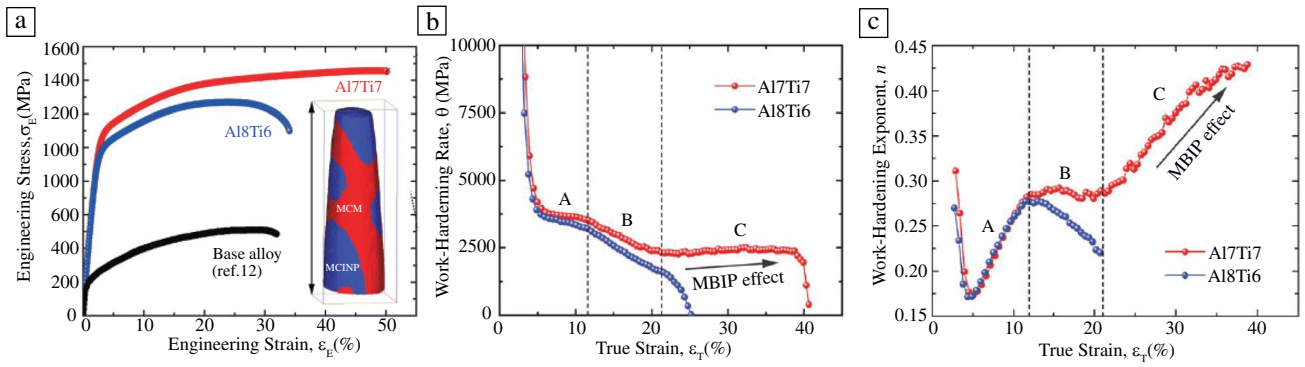

Figure 5. Strength, ductility, and strain hardening of intermetallic nanoparticles in a multicomponent matrix. (a) An $(FeCoNi)_{86}$-Al_7Ti_7 alloy consisting of ductile-ordered $L1_2$ intermetallic nanoparticles embedded in an fcc FeCoNi-matrix exhibited a σ_y of more than ~1 GPa, σ_{UTS} of ~1.5 GPa, and ε_f of ~50%. (b) Deformation-induced microbands enabling microband-induced plasticity (MBIP) resulted in multistage strain-hardening behavior. (c) The strain-hardening capacity with a strain-hardening exponent, *n,* up to 0.43 enabled continuous and stabilized plastic deformation and suppression of necking.[55]

who have designed an alloy consisting of a ductile disordered multicomponent matrix with ductile-ordered multicomponent intermetallic nanoparticles, briefly termed MCINP.[55] Through alloying an FeCoNi system with relatively large amounts of Ti and Al, $(FeCoNi)_{86}$-Al_7Ti_7, they introduce high-density $L1_2$ intermetallic nanoparticles in an fcc FeCoNi-base alloy system. The material, with uniform, equiaxed grains of ~40–50 mm and uniformly distributed ~30–50-nm-sized intermetallic nanoparticles, exhibits a tensile σ_y in excess of ~1 GPa, σ_{UTS} of ~1.5 GPa with ε_f of ~50%, as shown in **Figure** 5a. This is achieved through deformation-induced microbands enabling microband-induced plasticity (MBIP) in a multistage work-hardening behavior (Figure 5b), resulting in a work-hardening exponent, *n* up to 0.43 (Figure 5c).[55] The enhanced work-hardening capacity allows for continuous and stabilized plastic deformation, dislocation substructure formation, and dynamic Hall–Petch strengthening.

In 2020, the same group introduced alloys with superlattice structures that contain nanoscale-disordered interfaces between micrometer-scale superlattice grains, as schematically shown in **Figure** 6a.[56] The concept that is enabled in a $Ni_{43.9}Co_{22.4}Fe_{8.8}Al_{10.7}Ti_{11.7}B_{2.5}$ alloy, results in chemically ordered $L1_2$-structured ~11-µm-sized grains consisting of micrometer-scale ordered superlattice grains and a disordered interfacial layer. At the interface layer, Fe and Co partially replace Ni (Figure 6b), thereby decreasing the electron density of the ordered structure and suppressing the formation of brittle phases at grain boundaries. Simultaneously, disordered fcc nanolayers are formed along the interfaces of the B-enriched regions. The alloy shows a yield strength in tension of ~1 GPa, tensile strength in excess of 1.6 GPa, and failure strain of ~25%, as shown in Figure 6c. While these numbers are below those reported in the $(FeCoNi)_{86}$-Al_7Ti_7 alloy, it is important to note that high-temperature hardness tests reveal a pronounced resistance to thermal softening up to 800°C and only minor grain growth after 120 h at 1050°C. Such thermal stability clearly enables this material design concept for high-temperature structural applications.

However, due to their exceptional strength and the associated difficulty in making these $(FeCoNi)_{86}$-Al_7Ti_7 and $Ni_{43.9}Co_{22.4}Fe_{8.8}Al_{10.7}Ti_{11.7}B_{2.5}$ alloys in large sections, their fracture toughness behavior remains totally unexplored.

The most recent example of utilizing the versatile functions of multicomponent systems has recently been published in *Nature*.[57] In this work, the authors have designed a precipitate-strengthened FeNiAlTi (FNAT) MEA that not only strengthens the matrix phase of this alloy system but simultaneously modulates its transformation from fcc-austenite to bcc-martensite. During tensile testing, the matrix progressively transforms from austenite to martensite thereby increasing strength and ductility. As such, the dual functionality of the precipitates enables yield strengths of ~800 MPa together with extensive strain hardening resulting in outstanding combinations of strength and ductility. Furthermore, by altering precipitate characteristics such as size and spacing, as shown in atom probe tomography needles of both coarse- and fine-distributed precipitates in **Figure** 7a–b, respectively, strength and ductility can be tailored and controlled reliably allowing to achieve strength levels of 1.8 GPa and ductilities in excess of 40% failure strains (Figure 7c). While the resulting numbers do not rival those of the $(FeCoNi)_{86}$-Al_7Ti_7 alloy, it should be noted that this design concept not only demonstrates a dual functionality of microstructural components in a material but successfully illustrates the sequential activation of deformation mechanisms by tuning microstructure characteristics rather than composition.

The combinations of strength and ductility in these compositionally complex multi-phase M/HEAs are exceptional, and the obtained failure strains can be assumed to provide damage tolerance and resistance against premature failure. However,

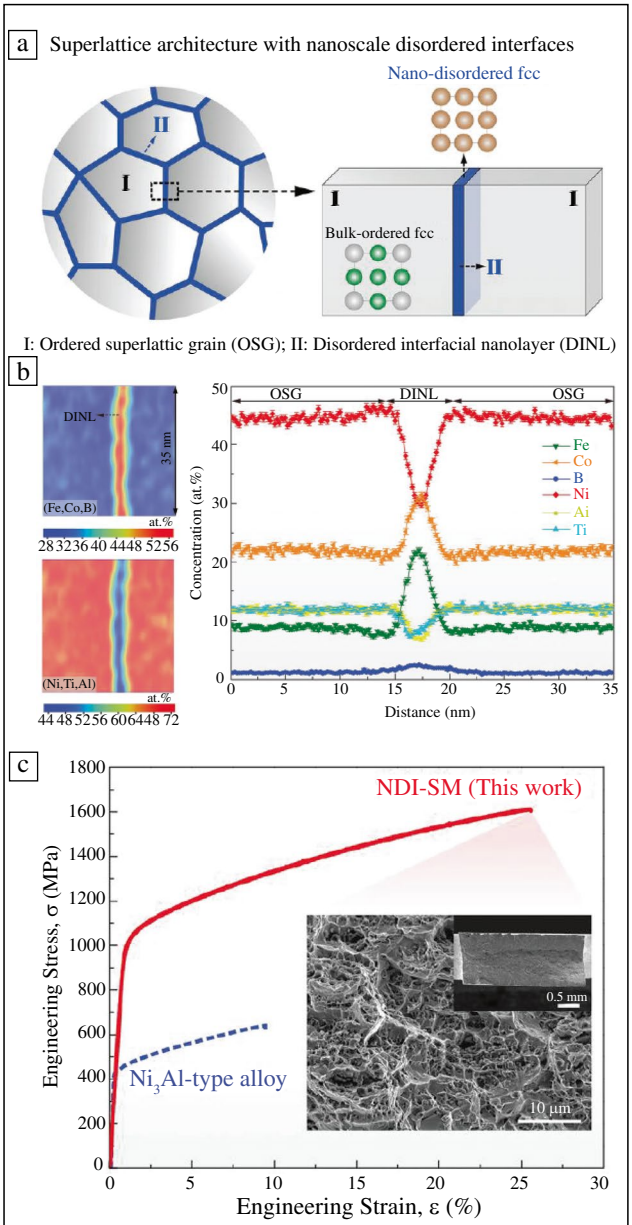

Figure 6. Damage tolerance of multicomponent superlattice materials. (a) A schematic showing the concept of alloys with superlattice structures that contain nanoscale-disordered interfaces between micrometer-scale superlattice grains. (b) In a $Ni_{43.9}Co_{22.4}Fe_{8.8}Al_{10.7}Ti_{11.7}B_{2.5}$ alloy, Fe and Co partially replace Ni at the interface that is additionally enriched in B. (c) Tensile stress–strain testing reveals a yield strength of ~ 1 GPa with tensile strength above 1.6 GPa and failure strains of more than 25%.[56]

as noted above, strength levels that are either comparable, or in many cases exceed, those of bcc RHEAs require further characterization of mechanical performance in terms of their deformation behavior and most especially their fracture resistance. In high-strength alloys with meticulously tailored mechanical performance properties, such as those mentioned above, decorated grain boundaries and/or high-density precipitates are known to often act as detrimental stress concentrations that result in the formation of cracks. Despite the successful suppression of necking through extensive strain hardening, mechanical performance in terms of failure characteristics of samples containing a crack has yet to be assessed to evaluate the full potential of these alloys as materials for damage-tolerant applications.

Ductility criteria

Since there is effectively an unlimited number of possible combinations of elements to form multiple principal element alloys that are yet to be explored, there have been numerous attempts to use computational techniques and/or experimental combinatorial procedures to find new and promising alloys. This is particularly true for the bcc RHEAs. While it is not too difficult to make predictions, find data, and/or make measurements on the strength/hardness properties of these alloys, the critical property is invariably their ductility, as extremely brittle alloys are clearly unsuitable for most structural applications.

There are nominally two predictive methodologies that can be used to estimate whether an alloy displays some ductility or is brittle, namely the use of the semi-empirical Pugh ratio[58] or the Rice–Thomson ductile versus brittle analysis.[59] Both approaches have been used to screen new high-entropy alloys for their likely ductility properties.[60,61]

The Pugh ratio is based on the ratio of the shear to bulk modulus, G/B, which needs to be small for ductile alloys on the assumption that a low G will promote plasticity whereas a high B will inhibit cavitation and the opening of cracks.[58] Analysis of numerous crystalline alloys suggests that if G/B exceeds roughly 0.6, the alloy is likely to be brittle. The Rice–Thomson analysis[59] is more fundamental and is directed to the behavior ahead of a crack (e.g., in mode I), it considers the competition of whether brittle cleavage, at a stress intensity K_{Ic}, or dislocation emission, at a stress intensity of K_{Ie}, will occur first at the crack tip. In principle, for a ductile material, $K_{Ie} < K_{Ic}$ and the emission of the dislocation serves to blunt the sharp crack tip; for an ideally brittle material, $K_{Ie} > K_{Ic}$, as per the Griffith theory. Calculating these respective stress intensities is not necessarily straightforward, but the analysis of Mak et al.[61] does suggest that there is a reasonable correlation between the calculated K_{Ie}/K_{Ic} ratios and the measured (compression) ductilities for a series of refractory alloys and RHEAs. Although it is necessary to consider the complications of mixed-mode loading and cleavage plane orientation, where the K_{Ie}/K_{Ic} ratio is low (typically less than 1.3 to 1.6, depending upon orientation), these alloys tend to display some ductility, whereas above these ratios they tend to be brittle.

These methods naturally take little account of microstructure and are still essentially correlations in nature, but they do present a means to screen numerous potential compositions before the expense of experimental testing. This is particularly

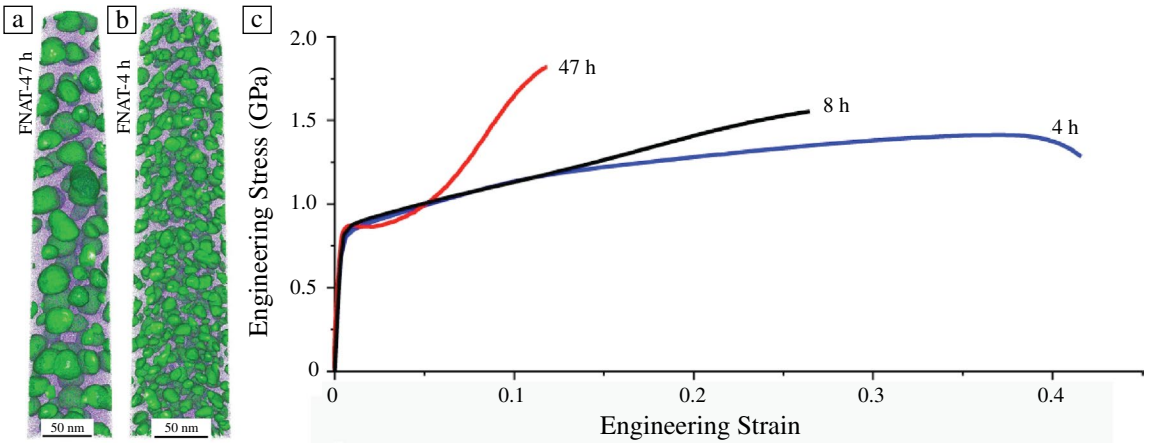

Figure 7. Dual functionality of an FeNiAlTi MEA. (a) Coarse- and (b) fine-distributed precipitates serve to strengthen the material while simultaneously modulating the transition of fcc-austenite to bcc-martensite. (c) After annealing heat treatments at 700°C between 4 and 47 h, the resulting materials exhibit yield strengths of ~ 800 MPa, tensile strengths up to ~ 1.8 GPa, and ductilities of more than ~ 40% failure strains.[57]

important for the refractory HEAs where the ductilities are markedly fracture limited.

Concluding remarks

Compositionally complex alloys including medium- and high-entropy alloys have revitalized the interest of researchers in metallic materials and alloy design for structural applications. This is evident from the rapid increase in journal publications in the past years with some outstanding discoveries highlighted in high-impact journals such as *Science* and *Nature*. While many of these articles present design strategies to simultaneously enhance strength and ductility, only a few concepts have proven to be that successful. Moreover, research characterizing fracture toughness and crack-resistance curve behavior, particularly under cyclic loading, is still very limited. For the successful design of structural materials, these properties, however, are necessary to fully understand damage tolerance and the true potential of a material that is considered for a structural application. For damage tolerance in materials that are deemed to operate at conditions such as at elevated temperatures beyond 1000°C, in radioactive or hydrogen environments, where the embrittlement of metals threatens safe operations and may stall the transformation into a future green energy production landscape, understanding strength and ductility alone will be insufficient and detailed characterization of the mechanisms underlying both deformation and fracture will be essential.

Acknowledgments

B.G. acknowledges support of the ARC Future Fellowship (Project No. FT190100484) and the UNSW Scientia Fellowship schemes. R.O.R. was supported by the US Department of Energy, Office of Science, Office of Basic Energy Sciences, Materials Sciences and Engineering Division under Contract No. DE-AC02-05-CH11231 within the Damage Tolerance in Structural Materials (KC 13) program at the Lawrence Berkeley National Laboratory.

Funding

Open Access funding enabled and organized by CAUL and its Member Institutions.

Conflict of interest

The authors state that there is no conflict of interest.

Open Access

References

1. A. Inoue, T. Zhang, T. Masumoto, *Mater. Trans. JIM* **30**, 965 (1989)
2. A. Inoue, H. Yamaguchi, T. Zhang, T. Masumoto, *Mater. Trans. JIM* **31**, 104 (1990)
3. C.J. Byrne, M. Eldrup, *Science* **321**, 502 (2008)
4. C.A. Schuh, T.C. Hufnagel, U. Ramamurty, *Acta Mater.* **55**, 4067 (2007)

5. C. Suryanarayana, A. Inoue, *Bulk Metallic Glasses*, 1st edn. (CRC Press, Baton Rouge, LA, 2010)
6. J.J. Kruzic, *Adv. Eng. Mater.* **18**, 1308 (2016)
7. K. Nomoto, A.V. Ceguerra, C. Gammer, B. Li, H. Bilal, A. Hohenwarter, B. Gludovatz, J. Eckert, S.P. Ringer, J.J. Kruzic, *Mater. Today* **44**, 48 (2021)
8. B. Cantor, I.T.H. Chang, P. Knight, A.J.B. Vincent, *Mater. Sci. Eng. A* **375–377**, 213 (2004)
9. J.-W. Yeh, S.-K. Chen, S.-J. Lin, J.-Y. Gan, T.-S. Chin, T.-T. Shun, C.-H. Tsau, S.-Y. Chang, *Adv. Eng. Mater.* **6**, 299 (2004)
10. C.-Y. Hsu, J.-W. Yeh, S.-K. Chen, T.-T. Shun, *Metall. Mater. Trans. A* **35**, 1465 (2004)
11. D.B. Miracle, O.N. Senkov, *Acta Mater.* **122**, 448 (2017)
12. E.P. George, D. Raabe, R.O. Ritchie, *Nat. Rev. Mater.* **4**, 515 (2019)
13. B. Gludovatz, E.P. George, R.O. Ritchie, *JOM* **67**, 2262 (2015)
14. A. Gali, E.P. George, *Intermetallics* **39**, 74 (2013)
15. F. Otto, A. Dlouhý, Ch. Somsen, H. Bei, G. Eggeler, E.P. George, *Acta Mater.* **61**, 5743 (2013)
16. B. Gludovatz, A. Hohenwarter, D. Catoor, E.H. Chang, E.P. George, R.O. Ritchie, *Science* **345**, 1153 (2014)
17. R. Zhang, S. Zhao, J. Ding, Y. Chong, T. Jia, C. Ophus, M. Asta, R.O. Ritchie, A.M. Minor, *Nature* **581**, 283 (2020)
18. X. Chen, Q. Wang, Z. Cheng, M. Zhu, H. Zhou, P. Jiang, L. Zhou, Q. Xue, F. Yuan, J. Zhu, X. Wu, E. Ma, *Nature* **592**, 712 (2021)
19. Y. Muniandy, M. He, M. Eizadjou, E.P. George, J.J. Kruzic, S.P. Ringer, B. Gludovatz, *Mater. Charact.* **180**, 111437 (2021)
20. R.O. Ritchie, *Nat. Mater.* **10**, 817 (2011)
21.E08 Committee, *E1820-13 Standard Test Method for Measurement of Fracture Toughness* (ASTM International, West Conshohocken, PA, 2013)
22. B. Gludovatz, A. Hohenwarter, K.V.S. Thurston, H. Bei, Z. Wu, E.P. George, R.O. Ritchie, *Nat. Commun.* **7**, 10602 (2016)
23. B. Schuh, B. Völker, J. Todt, K.S. Kormout, N. Schell, A. Hohenwarter, *Materials* **11**(5), 662 (2018)
24. G. Laplanche, A. Kostka, C. Reinhart, J. Hunfeld, G. Eggeler, E.P. George, *Acta Mater.* **128**, 292 (2017)
25. Z. Li, K.G. Pradeep, Y. Deng, D. Raabe, C.C. Tasan, *Nature* **534**, 227 (2016)
26. S.S. Sohn, A.K. da Silva, Y. Ikeda, F. Körmann, W. Lu, W.S. Choi, B. Gault, D. Ponge, J. Neugebauer, D. Raabe, *Adv. Mater.* **31**, 1807142 (2019)
27. H.S. Oh, S.J. Kim, K. Odbadrakh, W.H. Ryu, K.N. Yoon, S. Mu, F. Körmann, Y. Ikeda, C.C. Tasan, D. Raabe, T. Egami, E.S. Park, *Nat. Commun.* **10**, 2090 (2019)
28. K.V.S. Thurston, B. Gludovatz, A. Hohenwarter, G. Laplanche, E.P. George, R.O. Ritchie, *Intermetallics* **88**, 65 (2017)
29. K.V.S. Thurston, B. Gludovatz, Q. Yu, G. Laplanche, E.P. George, R.O. Ritchie, *J. Alloys Compd.* **794**, 525 (2019)
30. J. Rackwitz, Q. Yu, Y. Yang, G. Laplanche, E.P. George, A.M. Minor, R.O. Ritchie, *Acta Mater.* **200**, 351 (2020)
31. W.J. Mills, *Int. Mater. Rev.* **42**, 45 (1997)
32.M. Sokolov, J. Robertson, L. Snead, D. Alexander, P. Ferguson, M. James, S. Maloy, W. Sommer, G. Willcutt, M. Louthan, in *Eff. Radiat. Mater. 20th Intl. Symp.*, S. Rosinski, M. Grossbeck, T. Allen, A. Kumar, Eds. (ASTM International, West Conshohocken, PA, 2001), pp. 125–147
33. J.R. Strife, D.E. Passoja, *Metall. Trans. A* **11**, 1341 (1980)
34. C.K. Syn, J.W. Morris, S. Jin, *Metall. Trans. A* **7**, 1827 (1976)
35. A.W. Pense, R.D. Stout, *Weld. Res. Counc. Bull.* **205**, 1 (1975)
36. D.T. Read, R.P. Reed, *Cryogenics* **21**, 415 (1981)
37. R.D. Stout, S.J. Wiersma, in *Advances in Cryogenic Engineering Materials.*, R.P. Reed, A.F. Clark, Eds. (Springer, New York, 1986), pp. 389–395
38. Y. Shindo, K. Horiguchi, *Sci. Technol. Adv. Mater.* **4**, 319 (2003)
39. J.W. Sa, H.K. Kim, C.H. Choi, H.T. Kim, K.H. Hong, H.K. Park, J.S. Bak, K.W. Lee, E.T. Ha, *Twenty-First IEEE/NPS Symposium on Fusion Engineering SOFE 05* (IEEE, Knoxville, TN, September 26–29, 2005), pp. 1–4
40. O. Grässel, G. Frommeyer, C. Derder, H. Hofmann, *J. Phys. IV* **07**(C5), C5-383 (1997)
41. O. Grässel, L. Krüger, G. Frommeyer, L.W. Meyer, *Int. J. Plast.* **16**, 1391 (2000)
42. G. Frommeyer, U. Brüx, P. Neumann, *ISIJ Int.* **43**, 438 (2003)
43. L. Chen, Y. Zhao, X. Qin, *Acta Metall. Sin. (Engl. Lett.)* **26**, 1 (2013)
44. S. Chen, H.S. Oh, B. Gludovatz, S.J. Kim, E.S. Park, Z. Zhang, R.O. Ritchie, Q. Yu, *Nat. Commun.* **11**, 1 (2020)
45. O.N. Senkov, G.B. Wilks, D.B. Miracle, C.P. Chuang, P.K. Liaw, *Intermetallics* **18**, 1758 (2010)
46. O.N. Senkov, G.B. Wilks, J.M. Scott, D.B. Miracle, *Intermetallics* **19**, 698 (2011)
47. O.N. Senkov, J.M. Scott, S.V. Senkova, F. Meisenkothen, D.B. Miracle, C.F. Woodward, *J. Mater. Sci.* **47**, 4062 (2012)
48. O.N. Senkov, D.B. Miracle, K.J. Chaput, J.-P. Couzinie, *J. Mater. Res.* **33**, 3092 (2018)
49.M. Moschetti, A. Xu, B. Schuh, A. Hohenwarter, J.-P. Couzinié, J.J. Kruzic, D. Bhattacharyya, B. Gludovatz, *JOM* **72**, 130 (2020)
50. E.J. Pickering, A.W. Carruthers, P.J. Barron, S.C. Middleburgh, D.E.J. Armstrong, A.S. Gandy, *Entropy* **23**, 98 (2021)
51. O.N. Senkov, J.M. Scott, S.V. Senkova, D.B. Miracle, C.F. Woodward, *J. Alloys Compd.* **509**, 6043 (2011)
52. B. Schuh, B. Völker, J. Todt, N. Schell, L. Perrière, J. Li, J.P. Couzinié, A. Hohenwarter, *Acta Mater.* **142**, 201 (2018)
53. S. Wei, S.J. Kim, J. Kang, Y. Zhang, Y. Zhang, T. Furuhara, E.S. Park, C.C. Tasan, *Nat. Mater.* **19**(11), 1175 (2020)
54. I.-A. Su, K.-K. Tseng, J.-W. Yeh, B. El-Sayed, C.-H. Liu, S.-H. Wang, *Scr. Mater.* **206**, 114225 (2022)
55. T. Yang, Y.L. Zhao, Y. Tong, Z.B. Jiao, J. Wei, J.X. Cai, X.D. Han, D. Chen, A. Hu, J.J. Kai, K. Lu, Y. Liu, C.T. Liu, *Science* **362**, 933 (2018)
56. T. Yang, Y.L. Zhao, W.P. Li, C.Y. Yu, J.H. Luan, D.Y. Lin, L. Fan, Z.B. Jiao, W.H. Liu, X.J. Liu, J.J. Kai, J.C. Huang, C.T. Liu, *Science* **369**, 427 (2020)
57. Y. Yang, T. Chen, L. Tan, J.D. Poplawsky, K. An, Y. Wang, G.D. Samolyuk, K. Littrell, A.R. Lupini, A. Borisevich, E.P. George, Nature **595**, 245 (2021)
58. S.F. Pugh, *Philos. Mag. J. Sci.* **45**, 823 (1954)
59. J.R. Rice, R. Thomson, *Philos. Mag.* **29**, 73 (1974)
60. O.N. Senkov, D.B. Miracle, *Sci. Rep.* **11**, 4531 (2021)
61. E. Mak, B. Yin, W.A. Curtin, *J. Mech. Phys. Solids* **152**, 104389 (2021) □

Bernd Gludovatz is a Scientia Associate Professor and ARC Future Fellow in the School of Mechanical and Manufacturing Engineering at UNSW Sydney, Australia. He received both his MS and PhD degrees in Materials Science and Engineering at the University of Leoben, Austria, before working as a postdoctoral fellow at the Materials Sciences Division of the Lawrence Berkeley National Laboratory. His work focuses on the mechanisms underlying deformation, fracture and fatigue of advanced structural alloys, nature-inspired composites, and biological materials. Gludovatz can be reached by email at b.gludovatz@unsw.edu.au.

Robert O. Ritchie is the H.T. & Jessie Chua Distinguished Professor of Engineering in the Departments of Materials Science and Engineering and Mechanical Engineering at the University of California, Berkeley, and senior faculty scientist at the Lawrence Berkeley National Laboratory. He received his BA, MA, PhD, and ScD degrees in physics/materials science from the Universiy of Cambridge, UK, and is known for his research into the mechanics and mechanisms of fracture and fatigue of structural and biological materials. He is a member of the National Academy of Engineering, the UK Royal Academy of Engineering, and a foreign member of The Royal Society, London, the Russian Academy of Sciences, and the Royal Swedish Academy of Engineering Sciences. Ritchie can be reached by email at roritchie@lbl.gov.